DIFFRACTION

Jan Stienstra

Talk at workshop 'Coherent Sheaves and Mirror Symmetry', Cambridge, May 20-22, 2005

Talk at workshop 'Variations on Mahler's measure', Luminy, May 30 - June 3, 2005

related papers:

1. *Motives from Diffraction.*

   submitted for Proceedings of EAGER conference in honour of Jaap Murre (for his 75th birthday) september 2004

2. *Mahler Measure, Eisenstein Series and Dimers.*

   arXiv:math.NT/0502197

3. *Mahler Measure Variations, Eisenstein Series and Instanton Expansions.*

   arXiv:math.NT/0502193

MIRROR SYMMETRY

A-side	B-side
Calabi-Yau	Calabi-Yau
Fano	Landau-Ginzburg
Fukaya category	coherent sheaves
melting crystals/dimers	???
quivers	???

What is 'mirror' of

$$\boxed{\textit{melting crystals/dimers} \overset{\text{discrete approximation}}{\longrightarrow} CY}$$

DIFFRACTION AS MIRROR SYMMETRY:

Frauenhofer model for diffraction

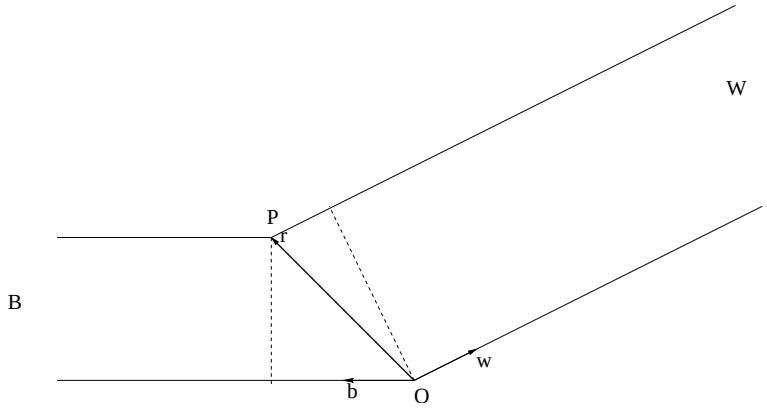

distance BW via P $=$ distance BW via $O - \langle \mathsf{b}{+}\mathsf{w}, \mathsf{r} \rangle$

$\rightsquigarrow$ phase difference $\rightsquigarrow$ multiply by factor $e^{-i\omega\langle \mathsf{b}+\mathsf{w},\mathsf{r}\rangle}$

Sum above over P in point configuration

$\approx$

Fouriertransform of point configuration

General set up

$$\boxed{\text{finite subset } \mathfrak{A} \subset \mathbb{Z}^n + \text{weights } c_{\mathsf{a}} \in \mathbb{N} \ (\mathsf{a} \in \mathfrak{A})}$$

$$=$$

$$\boxed{\text{distribution } \mathcal{D} \ = \ \sum_{\mathsf{a} \in \mathfrak{A}} c_{\mathsf{a}} \, \delta_{\mathsf{a}}}$$

$$\Longrightarrow \text{Fourier transform} \Longrightarrow$$

$$\boxed{\widehat{\mathcal{D}}(\mathsf{t}) = \sum_{\mathsf{a} \in \mathfrak{A}} c_{\mathsf{a}} e^{-2\pi i \langle \mathsf{t}, \mathsf{a} \rangle} \qquad \text{function on } \mathbb{R}^n}$$

$$\rightsquigarrow$$

$$\boxed{\text{diffraction pattern} = \text{level sets of } |\widehat{\mathcal{D}}(\mathsf{t})|^2}$$

$$\begin{aligned} |\widehat{\mathcal{D}}(\mathsf{t})|^2 \ &= \ \sum_{\mathsf{a},\mathsf{b} \in \mathfrak{A}} c_{\mathsf{a}} c_{\mathsf{b}} e^{2\pi i \langle \mathsf{t}, \mathsf{a}-\mathsf{b} \rangle} \\ &= \ \sum_{\mathsf{a},\mathsf{b} \in \mathfrak{A}} c_{\mathsf{a}} c_{\mathsf{b}} \cos(2\pi \langle \mathsf{t}, \mathsf{a} - \mathsf{b} \rangle) \end{aligned}$$

EXAMPLE
$\mathfrak{A} = \{(1,0),\ (0,1),\ (-1,-1)\} \subset \mathbb{Z}^2$,
$c_{(1,0)} = c_{(0,1)} = c_{(-1,-1)} = 1$.

Hence

$$|\widehat{\mathcal{D}}(t_1,t_2)|^2 \ = \ 3 + 2\cos(2\pi(t_1 - t_2)) + \\ +2\cos(2\pi(2t_1 + t_2)) + 2\cos(2\pi(t_1 + 2t_2))$$

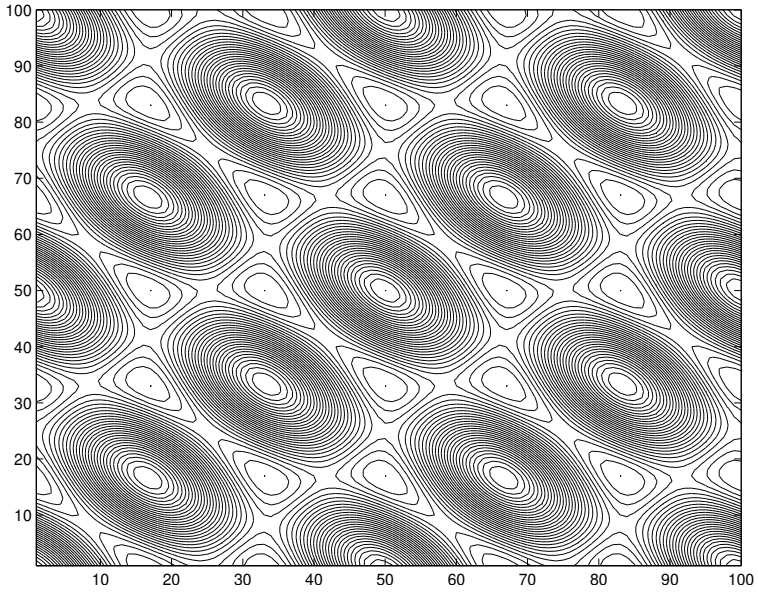

Diffraction pattern

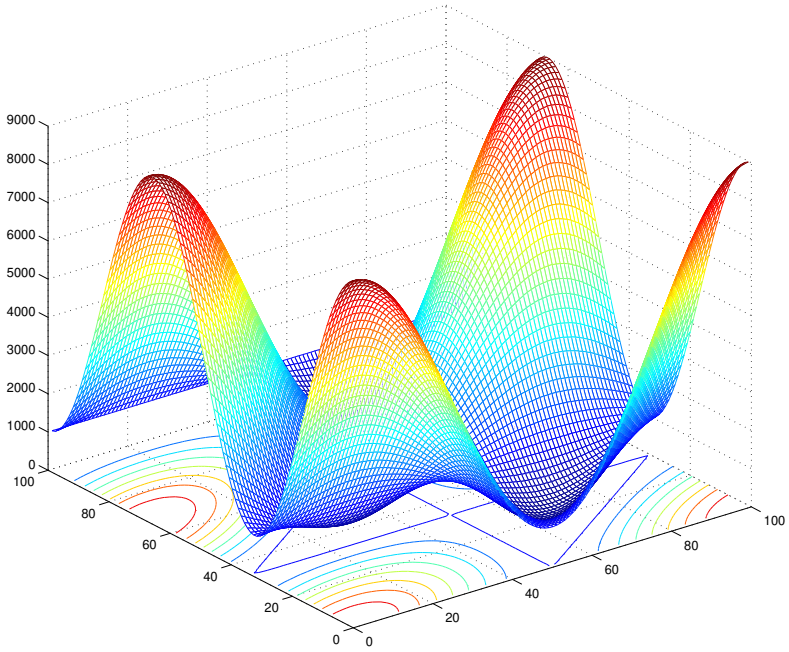
9000
8000
7000
6000
5000
4000
3000
2000
1000
0
100
80
60
40
20
0
0
20
40
60
80
100

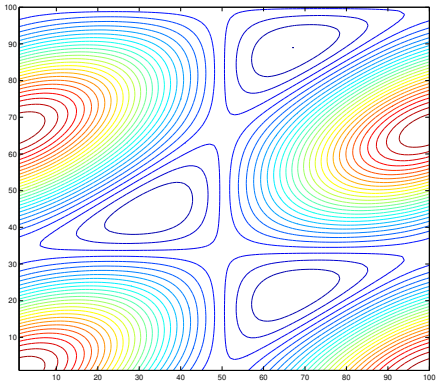
100
90
80
70
60
50
40
30
20
10
10
20
30
40
50
60
70
80
90
100

Function $|\widehat{\mathcal{D}}(\mathsf{t})|^2$ is periodic with period lattice $\Lambda^\vee$;

$$\begin{aligned}\Lambda^\vee &:= \{\mathsf{t} \in \mathbb{R}^n \mid \langle \mathsf{t}, \mathsf{a} - \mathsf{b}\rangle \in \mathbb{Z}\,,\ \forall \mathsf{a}, \mathsf{b} \in \mathfrak{A}\}\,,\\ \Lambda &:= \mathbb{Z}\text{–Span}\{\mathsf{a} - \mathsf{b} \mid \mathsf{a}, \mathsf{b} \in \mathfrak{A}\}.\end{aligned}$$

Assume Λ *has rank* n*.*

Introduce enumerative data (for $N \in \mathbb{N}$, $r \in \mathbb{R}$)

$$\text{mult}_N(r) := \sharp\{\mathsf{t} \in \tfrac{1}{N}\Lambda^\vee \,/\, \Lambda^\vee \mid |\widehat{\mathcal{D}}(\mathsf{t})|^2 \,=\, r\ \}$$

$N^{-n}\,\text{mult}_N(r)$ is a density on $\mathbb{R}$ with *moments*

$$\mathsf{m}_k^{(N)} \,:=\, N^{-n} \sum_r\, r^k\, \text{mult}_N(r)\,.$$

Encode data $\mathrm{mult}_N(r)$ as

$$\mathsf{B}_N(z) := \prod_{r\in\mathbb{R}} (z-r)^{\mathrm{mult}_N(r)}\,.$$

$\mathsf{B}_N(z)$ is a polynomial with coefficients in $\mathbb{Z}$.

EXAMPLE
$\mathfrak{A} = \{(1,0),\,(0,1),\,(-1,-1)\} \subset \mathbb{Z}^2$,
$c_{(1,0)} = c_{(0,1)} = c_{(-1,-1)} = 1$.

$$\begin{aligned}
\mathsf{B}_1 &= (z-9)\\
\mathsf{B}_2 &= (z-9)(z-1)^3\\
\mathsf{B}_3 &= (z-9)(z-3)^6 z^2\\
\mathsf{B}_4 &= (z-9)(z-5)^6(z-1)^9\\
\mathsf{B}_5 &= (z-9)(z^2-8z+11)^6(z^2-3z+1)^6\\
\mathsf{B}_6 &= (z-9)(z-7)^6(z-4)^6(z-3)^6(z-1)^{15}z^2\\
\mathsf{B}_7 &= (z-9)(z-2)^{12}(z^3-13z^2+47z-43)^6\times\\
&\qquad\qquad \times(z^3-6z^2+5z-1)^6
\end{aligned}$$

Substitution

$$x_j \;=\; e^{2\pi i t_j}$$

transforms $|\widehat{\mathcal{D}}(\mathsf{t})|^2$ to Laurent polynomial

$$W(x_1,\ldots,x_n) \;=\; \sum_{\mathsf{a},\mathsf{b}\in\mathfrak{A}} c_{\mathsf{a}} c_{\mathsf{b}} \mathsf{x}^{\mathsf{a}-\mathsf{b}} \;\in \mathbb{Z}[x_1^{\pm 1},\ldots,x_n^{\pm 1}]$$

Laurent polynomials are familiar objects in toric mirror symmetry and Landau-Ginzburg models!!

Special feature of above W:

$$W(x_1^{-1},x_2^{-1},\ldots,x_n^{-1}) \;=\; W(x_1,x_2,\ldots,x_n)$$

W is real valued function on real torus

$$\mathbb{U}^{\Lambda} := \mathrm{Hom}(\Lambda,\mathbb{U}) \qquad\qquad (\mathbb{U} := \{z\in\mathbb{C}\,|\,|z|=1\})\,.$$

$W(\mathbb{U}^{\Lambda})$ is compact interval $\mathcal{I} \;\subset\; \mathbb{R}$.

EXAMPLE
$\mathfrak{A} = \{(1,0),\, (0,1),\, (-1,-1)\},\ \forall c_{\mathsf{a}} = 1$

$$W(x_1, x_2) \;=\; (x_1 + x_2 + x_1^{-1}x_2^{-1})(x_1^{-1} + x_2^{-1} + x_1 x_2)$$

Basis $\{(2,1),\, (-1,-2)\}$ for the lattice Λ gives coordinates $u_1 = x_1^2 x_2$ and $u_2 = x_1^{-1}x_2^{-2}$ on torus $\mathbb{U}^\Lambda$

In these coordinates

$$\begin{aligned} W(u_1, u_2) \;&=\; (u_1 + u_2 + 1)(u_1^{-1} + u_2^{-1} + 1) \\ &=\; u_1 + u_1^{-1} + u_2 + u_2^{-1} + u_1^{-1}u_2 + u_1 u_2^{-1} + 3\,. \end{aligned}$$

Triangulated Newton polygon of W:

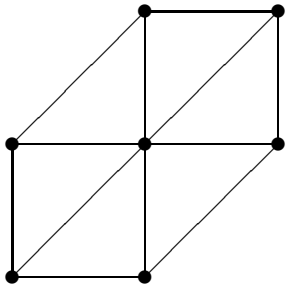

is toric diagram for Del Pezzo surface dP_3.

Using the Laurent polynomial W we can write

$$\mathsf{B}_N(z) = \prod_{\mathsf{x} \in \mu_N^\Lambda} (z - W(\mathsf{x}))\,,$$

with

$$\mu_N^\Lambda := \mathrm{Hom}(\Lambda, \mu_N) \qquad\qquad (\mu_N := \{z \in \mathbb{C} \mid z^N = 1\})\,.$$

This shows that $\mathsf{B}_N(z) \in \mathbb{Z}[z]$.

Consider the function $\mathsf{Q} : \mathbb{C} \setminus \mathcal{I} \longrightarrow \mathbb{R}_{>0}$

$$\mathsf{Q}(z) = \exp\left(\frac{-1}{(2\pi i)^n} \int_{\mathbb{U}^n} \log|z - W(x_1, \ldots, x_n)| \, \frac{dx_1}{x_1} \, \ldots \, \frac{dx_n}{x_n}\right)$$

$\mathsf{Q}(z)^{-1}$ is the *Mahler measure* of the Laurent polynomial $z - W$.

For real $z > \max \mathcal{I}$

$$\boxed{\lim_{N\to\infty} \, |\mathsf{B}_N(z)|^{-N^{-n}} \; = \; \mathsf{Q}(z)}$$

For real $z > \max \mathcal{I}$

$$\boxed{\lim_{N\to\infty} \; |\mathsf{B}_N(z)|^{-N^{-n}} \;=\; \mathsf{Q}(z)}$$

proof:

$$\log |\mathsf{B}_N(z)|^{-N^{-n}} \;=\; -\log z \;+\; \sum_{k\geq 1} \mathsf{m}_k^{(N)} \frac{z^{-k}}{k}$$

with

$$\mathsf{m}_k^{(N)} = N^{-n} \sum_{\mathsf{x}\in\mu_N^{\Lambda}} W(\mathsf{x})^k$$

So: $\mathsf{m}_k^{(N)}$ is the sum of the coefficients of those monomials in W^k for which the exponent is in $N\Lambda$.

$$\log \mathsf{Q}(z) \;=\; -\log z \;+\; \sum_{k\geq 1} \mathsf{m}_k \frac{z^{-k}}{k}$$

with

$$\mathsf{m}_k := \frac{1}{(2\pi i)^n} \int_{\mathbb{U}^n} W(\mathsf{x})^k \, \frac{dx_1}{x_1} \, \ldots \, \frac{dx_n}{x_n}$$

So: m_k is the constant term of W^k.

$$\begin{array}{rcl} W(1)^k & \geq & \mathsf{m}_k^{(N)} \;\geq\; \mathsf{m}_k \;\geq\; 0 \qquad \text{for all} \qquad N,\, k\,, \\ \mathsf{m}_k^{(N)} & = & \mathsf{m}_k \qquad \text{if} \quad N > k \max_{\mathsf{a},\mathsf{b}\in\mathfrak{A},\, 1\leq j\leq n} |a_j - b_j|\,. \end{array}$$

■

EXAMPLE
$\mathfrak{A} = \{(1,0),\, (0,1),\, (-1,-1)\},\ \forall c_{\mathsf{a}} = 1.$

$$\mathsf{m}_k \;=\; \sum_{j=0}^{k} \left(\begin{array}{c} k \\ j \end{array} \right)^2 \left(\begin{array}{c} 2j \\ j \end{array} \right) .$$

$$\mathsf{m}_k^{(N)} \;=\; \sum_{i_1 \equiv i_2 \bmod N,\, j_1 \equiv j_2 \bmod N} \left(\begin{array}{c} k \\ i_1 \end{array} \right) \left(\begin{array}{c} k - i_1 \\ j_1 \end{array} \right) \times \\ \times \left(\begin{array}{c} k \\ i_2 \end{array} \right) \left(\begin{array}{c} k - i_2 \\ j_2 \end{array} \right)$$

These formulas confirm $\mathsf{m}_k^{(N)} = \mathsf{m}_k$ for $k < N$.

EXAMPLE
$\mathfrak{A} = \{(1,0),\, (0,1),\, (-1,-1)\},\ \forall c_{\mathsf{a}} = 1.$

The numbers m_k $(k \geq 0)$ satisfy the recurrence

$$(k+1)^2 \mathsf{m}_{k+1} = (10k^2 + 10k + 3)\mathsf{m}_k - 9k^2 \mathsf{m}_{k-1}\,.$$

This recurrence is equivalent to the Picard-Fuchs differential equation for

$$z\frac{d}{dz}\log \mathsf{Q}(z)\,.$$

refer to Golyshev's talk for:
Picard-Fuchs $\rightsquigarrow$ quantum cohomology of dP_3.

refer to my paper *Mahler Measure Variations, Eisenstein Series and Instanton Expansions* for:
Picard-Fuchs $\rightsquigarrow$ instanton counts for dP_3.

BIPARTITE GRAPH

Assume $\mathfrak{A} \cap \Lambda = \emptyset$.

Construct a Λ-periodic weighted bipartite graph Γ:

$$\{\text{black vertices of } \Gamma\} = \Lambda$$
$$\{\text{white vertices of } \Gamma\} = \mathfrak{A} + \Lambda$$

$$\{\text{edges of } \Gamma\} = \{(\mathsf{v}_1, \mathsf{v}_2) \in \Lambda \times (\mathfrak{A} + \Lambda) \mid \mathsf{v}_2 - \mathsf{v}_1 \in \mathfrak{A}\}$$
$$\text{weight}(\mathsf{v}_1, \mathsf{v}_2) = c_{\mathsf{a}} \qquad \text{iff} \qquad \mathsf{v}_2 - \mathsf{v}_1 = \mathsf{a} \in \mathfrak{A}$$

Then

$$\frac{N^n}{k} \mathsf{m}_k^{(N)} = \sharp\{\text{closed paths of length } 2k \text{ on } \Gamma \,/\, N\Lambda\}$$

(paths are counted with weights!)

Note:
The input data $(\mathfrak{A}, c_{\mathsf{a}})$ can directly be recovered from the embedding of Γ in $\mathbb{R}^n$ (plus weights).
The diffraction pattern is not the Fouriertransform of Γ!

EXAMPLE
$\mathfrak{A} = \{(1,0),\, (0,1),\, (-1,-1)\} \subset \mathbb{Z}^2$,
$c_{(1,0)} = c_{(0,1)} = c_{(-1,-1)} = 1$.

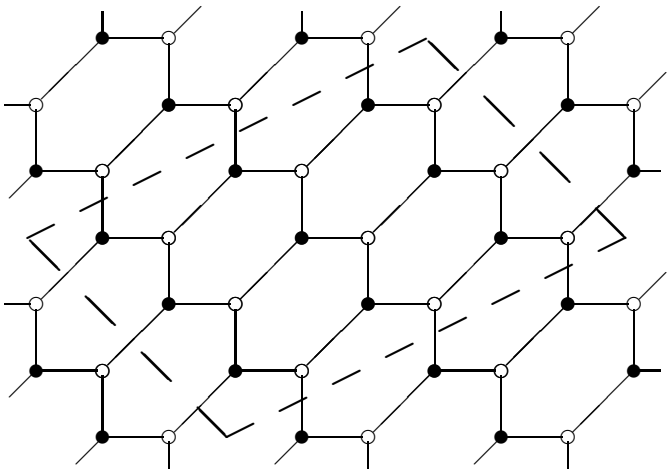

A fundamental parallelogram of the lattice 3Λ *and a piece of the bipartite graph* Γ.
All edges have weight 1.
By identifying opposite sides of the parallelogram one obtains the graph $\Gamma \,/\, 3\Lambda$.

DIMER CONFIGURATIONS ON Γ / 3Λ

From now on $\mathfrak{A} = \{(1,0), (0,1), (-1,-1)\}$, $\forall c_{\mathsf{a}} = 1$.

Γ = corresponding bipartite graph.

A *dimer configuration*, or perfect matching, on the graph Γ / 3Λ is a collection $\mathcal{M}$ of its edges such that each vertex of Γ / 3Λ is incident to exactly one edge from $\mathcal{M}$.

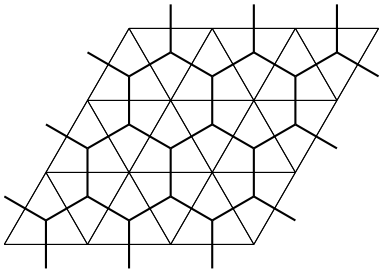

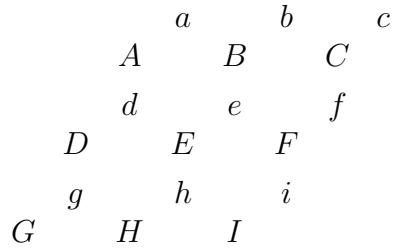

$$\mathsf{K} := \begin{bmatrix} Aa & Ba & 0 & 0 & 0 & 0 & Ga*x & 0 & 0 \\ 0 & Bb & Cb & 0 & 0 & 0 & 0 & Hb*x & 0 \\ Ac*y & 0 & Cc & 0 & 0 & 0 & 0 & 0 & Ic*x \\ Ad & 0 & 0 & Dd & Ed & 0 & 0 & 0 & 0 \\ 0 & Be & 0 & 0 & Ee & Fe & 0 & 0 & 0 \\ 0 & 0 & Cf & Df*y & 0 & Ff & 0 & 0 & 0 \\ 0 & 0 & 0 & Dg & 0 & 0 & Gg & Hg & 0 \\ 0 & 0 & 0 & 0 & Eh & 0 & 0 & Hh & Ih \\ 0 & 0 & 0 & 0 & 0 & Fi & Gi*y & 0 & Ii \end{bmatrix}.$$

Matrix entries used as abstract weights on the graph edges. $*x$ (resp. $*y$) marks the graph edges for which the top-bottom (resp. left-right) sides of the fundamental parallellogram must be identified.

K is the matrix of the *Kasteleijn operator* of the dimer model on $\Gamma/3\Lambda$. The determinant

$$P(x, y) := \det \mathsf{K}$$

is called the *characteristic polynomial* of the dimer model.

The curve

$$\{(x, y) \in \mathbb{C}^* \times \mathbb{C}^* \mid P(x, y) = 0\}$$

is called the *spectral curve* of the dimer model.

Each dimer configuration appears exactly once in $\det \mathsf{K}$ through the product of its (abstract) weights (e.g. $Fi * Eh * Dg * Cf * Be * Ad * Ic * Hb * Ga$).

A dimer configuration is a bijective map from black to white vertices and can be denoted as $\begin{bmatrix} i\,h\,g\,f\,e\,d\,c\,b\,a \\ FEDCBAIHG \end{bmatrix}$.

$$Z^3P(\tfrac{X}{Z},\tfrac{Y}{Z}) =$$

$$X^3\begin{bmatrix} i & h & g & f & e & d & c & b & a \\ F & E & D & C & B & A & I & H & G \end{bmatrix} + Y^3\begin{bmatrix} i & h & g & f & e & d & c & b & a \\ G & I & H & D & F & E & A & C & B \end{bmatrix} + Z^3\begin{bmatrix} i & h & g & f & e & d & c & b & a \\ I & H & G & F & E & D & C & B & A \end{bmatrix}$$

$$+XZ^2(\begin{bmatrix} i & h & g & f & e & d & c & b & a \\ F & H & G & C & E & D & I & B & A \end{bmatrix} + \begin{bmatrix} i & h & g & f & e & d & c & b & a \\ I & E & G & F & B & D & C & H & A \end{bmatrix} + \begin{bmatrix} i & h & g & f & e & d & c & b & a \\ I & H & D & F & E & A & C & B & G \end{bmatrix})$$

$$+X^2Z(\begin{bmatrix} i & h & g & f & e & d & c & b & a \\ F & E & G & C & B & D & I & H & A \end{bmatrix} + \begin{bmatrix} i & h & g & f & e & d & c & b & a \\ F & H & D & C & E & A & I & B & G \end{bmatrix} + \begin{bmatrix} i & h & g & f & e & d & c & b & a \\ I & E & D & F & B & A & C & H & G \end{bmatrix})$$

$$+YZ^2(\begin{bmatrix} i & h & g & f & e & d & c & b & a \\ G & I & H & F & E & D & C & B & A \end{bmatrix} + \begin{bmatrix} i & h & g & f & e & d & c & b & a \\ I & H & G & D & F & E & C & B & A \end{bmatrix} + \begin{bmatrix} i & h & g & f & e & d & c & b & a \\ I & H & G & F & E & D & A & C & B \end{bmatrix})$$

$$+Y^2Z(\begin{bmatrix} i & h & g & f & e & d & c & b & a \\ G & I & H & D & F & E & C & B & A \end{bmatrix} + \begin{bmatrix} i & h & g & f & e & d & c & b & a \\ G & I & H & F & E & D & A & C & B \end{bmatrix} + \begin{bmatrix} i & h & g & f & e & d & c & b & a \\ I & H & G & D & F & E & A & C & B \end{bmatrix})$$

$$+X^2Y(\begin{bmatrix} i & h & g & f & e & d & c & b & a \\ G & E & D & C & F & A & I & H & B \end{bmatrix} + \begin{bmatrix} i & h & g & f & e & d & c & b & a \\ F & E & H & D & B & A & I & C & G \end{bmatrix} + \begin{bmatrix} i & h & g & f & e & d & c & b & a \\ F & I & D & C & B & E & A & H & G \end{bmatrix})$$

$$+XY^2(\begin{bmatrix} i & h & g & f & e & d & c & b & a \\ G & E & H & D & F & A & I & C & B \end{bmatrix} + \begin{bmatrix} i & h & g & f & e & d & c & b & a \\ G & I & D & C & F & E & A & H & B \end{bmatrix} + \begin{bmatrix} i & h & g & f & e & d & c & b & a \\ F & I & H & D & B & E & A & C & G \end{bmatrix})$$

$$\begin{aligned} -XYZ(&\begin{bmatrix} i & h & g & f & e & d & c & b & a \\ G & E & H & C & F & D & I & B & A \end{bmatrix} + \begin{bmatrix} i & h & g & f & e & d & c & b & a \\ G & H & D & C & F & E & I & B & A \end{bmatrix} + \begin{bmatrix} i & h & g & f & e & d & c & b & a \\ G & E & H & F & B & D & I & C & A \end{bmatrix} \\ &+ \begin{bmatrix} i & h & g & f & e & d & c & b & a \\ F & H & G & D & B & E & I & C & A \end{bmatrix} + \begin{bmatrix} i & h & g & f & e & d & c & b & a \\ G & H & D & F & B & E & I & C & A \end{bmatrix} + \begin{bmatrix} i & h & g & f & e & d & c & b & a \\ F & I & G & D & B & E & C & H & A \end{bmatrix} \\ &+ \begin{bmatrix} i & h & g & f & e & d & c & b & a \\ G & I & D & F & B & E & C & H & A \end{bmatrix} + \begin{bmatrix} i & h & g & f & e & d & c & b & a \\ F & H & G & D & E & A & I & C & B \end{bmatrix} + \begin{bmatrix} i & h & g & f & e & d & c & b & a \\ G & H & D & F & E & A & I & C & B \end{bmatrix} \\ &+ \begin{bmatrix} i & h & g & f & e & d & c & b & a \\ F & I & G & C & E & D & A & H & B \end{bmatrix} + \begin{bmatrix} i & h & g & f & e & d & c & b & a \\ I & E & G & C & F & D & A & H & B \end{bmatrix} + \begin{bmatrix} i & h & g & f & e & d & c & b & a \\ F & I & G & D & E & A & C & H & B \end{bmatrix} \\ &+ \begin{bmatrix} i & h & g & f & e & d & c & b & a \\ G & I & D & F & E & A & C & H & B \end{bmatrix} + \begin{bmatrix} i & h & g & f & e & d & c & b & a \\ I & E & G & D & F & A & C & H & B \end{bmatrix} + \begin{bmatrix} i & h & g & f & e & d & c & b & a \\ F & I & H & C & E & D & A & B & G \end{bmatrix} \\ &+ \begin{bmatrix} i & h & g & f & e & d & c & b & a \\ I & E & H & C & F & D & A & B & G \end{bmatrix} + \begin{bmatrix} i & h & g & f & e & d & c & b & a \\ I & H & D & C & F & E & A & B & G \end{bmatrix} + \begin{bmatrix} i & h & g & f & e & d & c & b & a \\ F & I & H & D & E & A & C & B & G \end{bmatrix} \\ &+ \begin{bmatrix} i & h & g & f & e & d & c & b & a \\ I & E & H & D & F & A & C & B & G \end{bmatrix} + \begin{bmatrix} i & h & g & f & e & d & c & b & a \\ I & E & H & F & B & D & A & C & G \end{bmatrix} + \begin{bmatrix} i & h & g & f & e & d & c & b & a \\ I & H & D & F & B & E & A & C & G \end{bmatrix}). \end{aligned}$$

We now want to substitute the abstract weights by 0 or 1 such that the characteristic polynomial becomes

$$X^2Y + XY^2 + X^2Z + XZ^2 + Y^2Z + YZ^2 - tXYZ$$

for some $t \in \mathbb{Z}$.

SOLUTION 1:
$Aa = Fi = Hg = 0$, all others $= 1$, yields $\quad t = 6$.

SOLUTION 2:
$Aa = Be = Ih = 0$, all others $= 1$, yields $\quad t = 7$.

SOLUTION 3:
$Aa = Be = Hg = 0$, all others $= 1$, yields $\quad t = 8$.

SOLUTION 4:
$Aa = Be = Ed = 0$, all others $= 1$, yields $\quad t = 11$.

NOTE:

$$\begin{aligned} & X^2Y + XY^2 + X^2Z + XZ^2 + Y^2Z + YZ^2 - tXYZ \\ = \; & (X+Y+Z)(XY+YZ+ZX) - (3+t)XYZ \end{aligned}$$

So, the spectral curves of the above dimer models are not visible in the intersection pattern (except for one point in solution 1)

SOLUTION 1:

$Aa = Fi = Hg = 0$, all others $= 1$, yields $t = 6$.

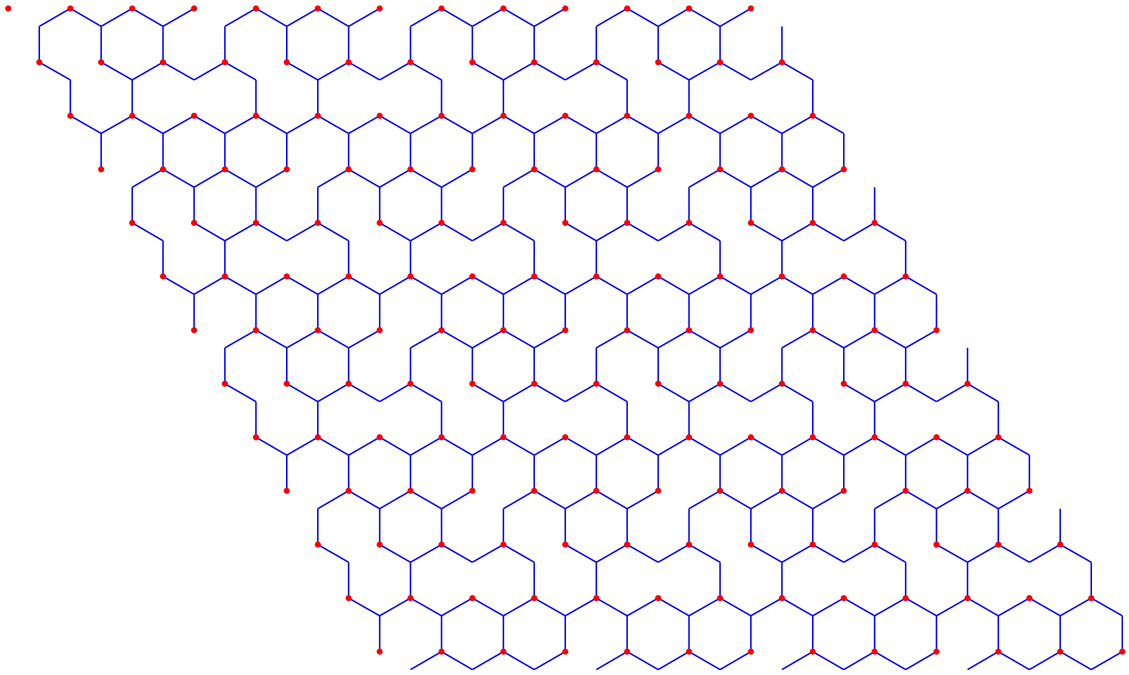

SOLUTION 2:

$Aa = Be = Ih = 0$, all others $= 1$, yields $\quad t = 7.$

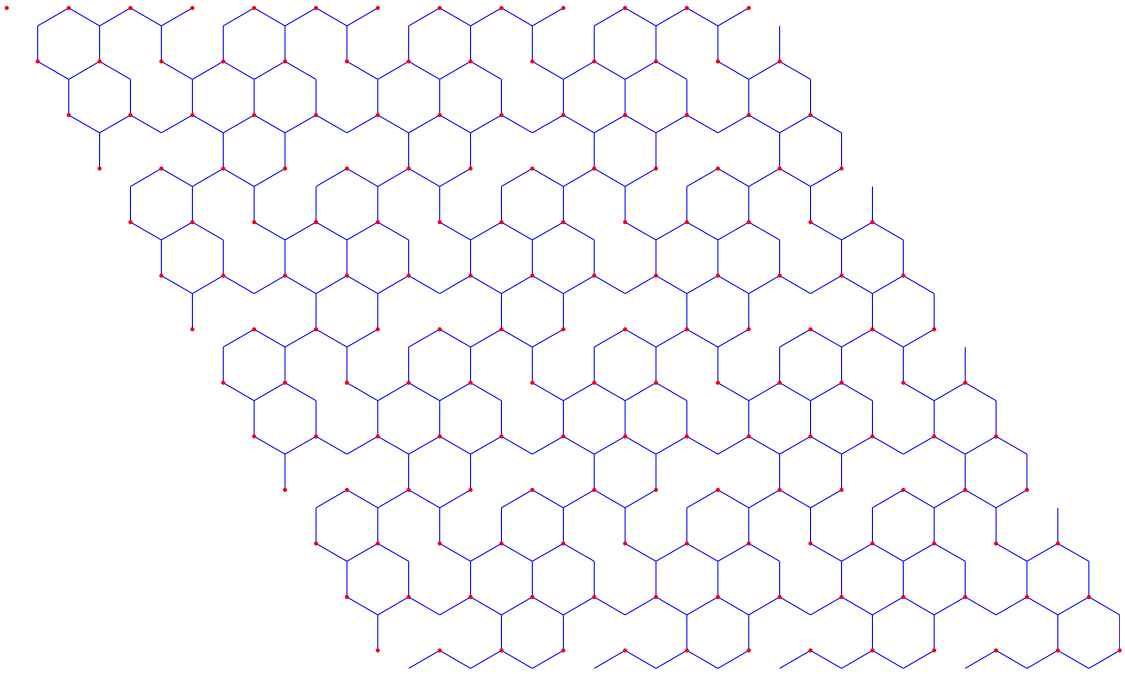

SOLUTION 3:

$Aa = Be = Hg = 0$, all others $= 1$, yields $t = 8$.

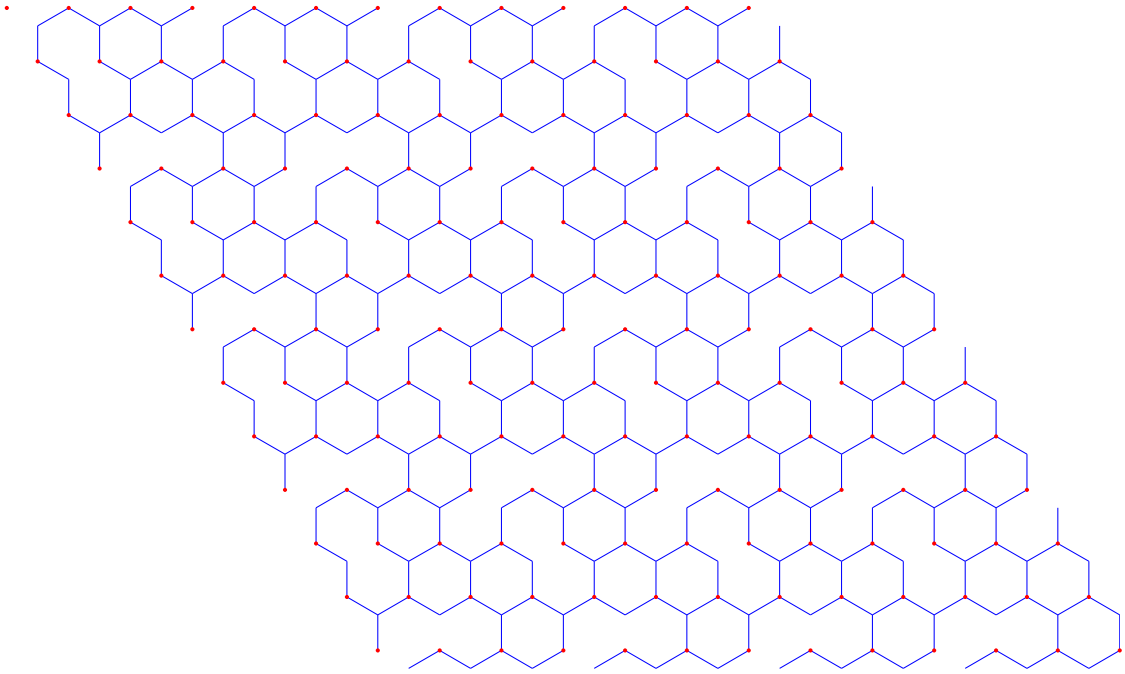

SOLUTION 4:

$Aa = Be = Ed = 0$, all others $= 1$, yields $t = 11$.

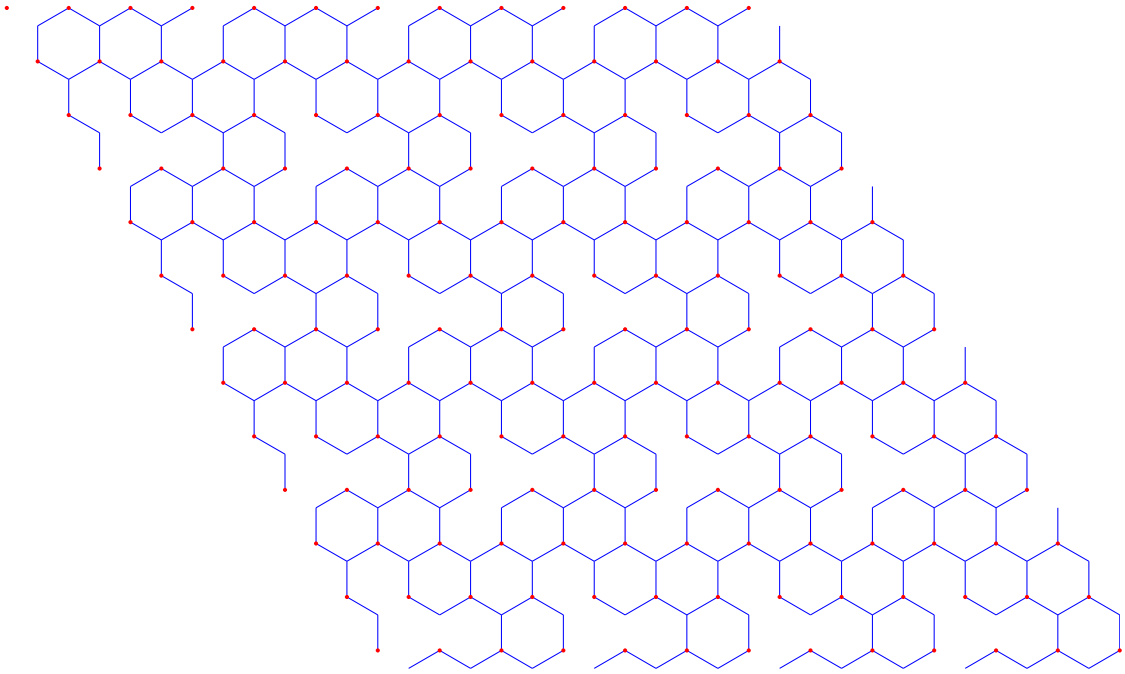

three valence 4 and two valence 3 nodes. It also contains twelve edges, corresponding to the twelve bifundamental fields in the quiver.

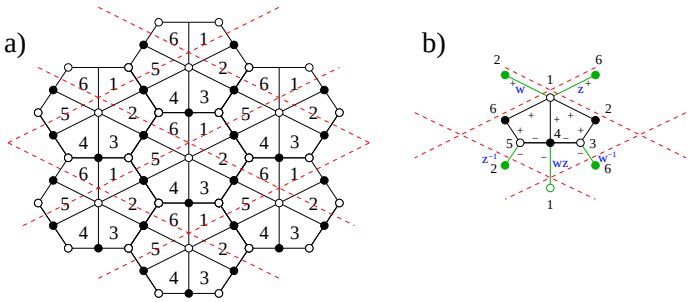

Figure 4: a) Brane tiling for Model I of $\mathbf{dP}_3$ with flux lines indicated in red. b) Unit cell for Model I of $\mathbf{dP}_3$. We show the edges connecting to images of the fundamental nodes in green. We also indicate the signs associated to each edge as well as the powers of w and z corresponding to crossing flux lines.

From the unit cell, we derive the following Kasteleyn matrix

$$K = \begin{pmatrix} & 2 & 4 & 6 \\ \hline 1 & 1+w & 1-zw & 1+z \\ 3 & 1 & -1 & -w^{-1} \\ 5 & -z^{-1} & -1 & 1 \end{pmatrix} \tag{3.4}$$

We observe that is has twelve monomials, associated to the twelve bifundamental fields. This matrix leads to the characteristic polynomial

$$P(z,w) = w^{-1}z^{-1} - z^{-1} - w^{-1} - 6 - w - z + wz. \tag{3.5}$$

The toric data corresponding to this gauge theory can be read from this polynomial, and is shown in Figure 5.

The Kasteleyn matrix is a square matrix whose size is equal to half the total number of points in the unit cell. Thus, for a given toric quiver K is a $N_W/2 \times N_W/2$ matrix. This is remarkable, since this size can be very modest even for very complicated gauge theories. The simplicity of computing the toric data using this procedure should be contrasted with the difficulty of the Forward Algorithm.

actions (rotations and reflections) on them; this is what we mean by quiver automorphism. Now let us move on to see how the symmetry determines the superpotentials.

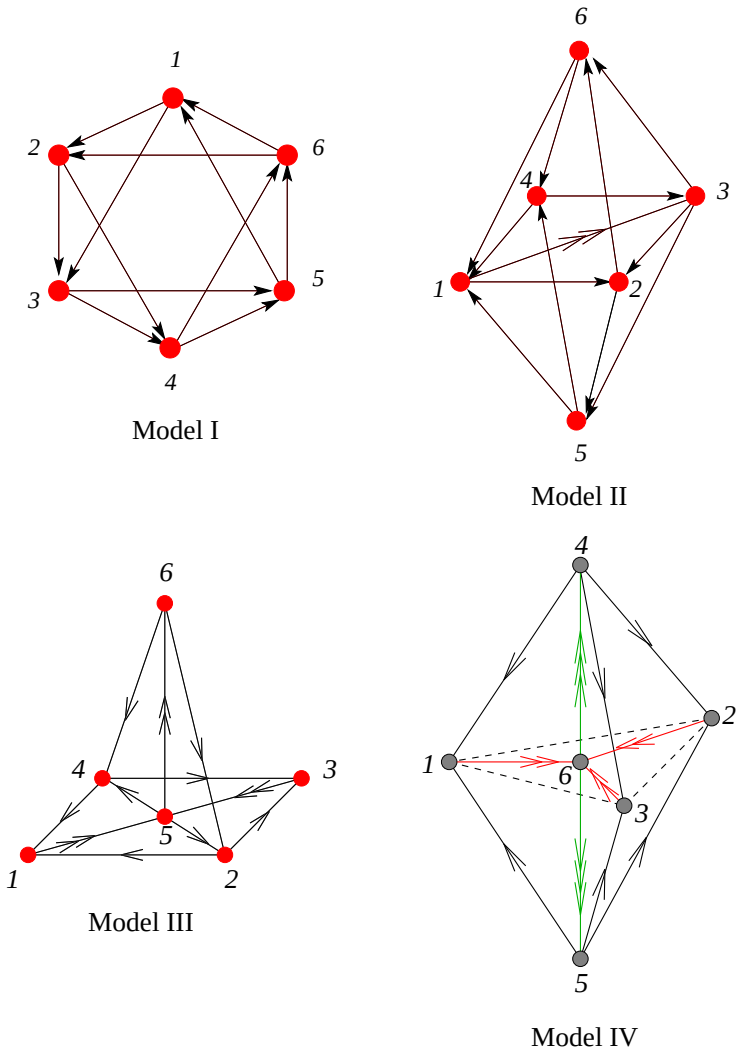

Figure 9: Quiver diagrams of the four torically dual theories corresponding to the cone over dP_3. We see explicitly the node symmetries to be respectively: D_6, $\mathbb{Z}_2 \times \mathbb{Z}_2$, $\mathbb{Z}_2 \times \mathbb{Z}_2$ and D_6.

Let us first focus on model I. We see that its quiver exhibits a D_6 symmetry of the Star of David. This quiver has the following closed loops (i.e. gauge invariant operators): one loop with six fields, six loops with five fields, nine loops with four fields and two loops with three fields. Our basic idea is following:

- If a given loop is contained in the superpotential, all its images under the node symmetry group also have to be present;

Del Pezzo 3

There are four toric phases for $\mathbf{dP}_3$. We refer the reader to [13] for their quivers and superpotentials. We have already presented the tiling for Model I in Figure 1. Its Kasteleyn matrix and characteristic polynomial are written in (3.4) and (3.5). Figure 18 shows the tiling for Model II. Its Kasteleyn matrix and characteristic polynomial are presented in (8.3) and (8.4). We now proceed with the construction of the brane tilings for Models III and IV.

Model III

We show the brane tiling in Figure 23. The Kasteleyn matrix is

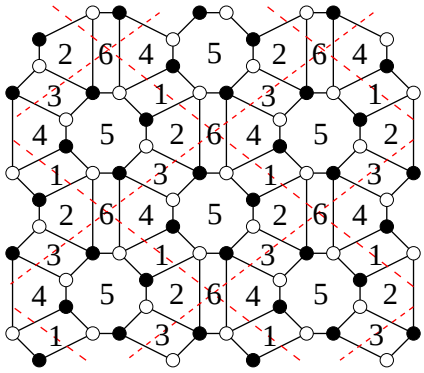

Figure 23: Brane tiling for Model III of $\mathbf{dP}_3$.

$$K = \left(\begin{array}{c|cccc} & 2 & 4 & 6 & 8 \\ \hline 1 & 1 & w^{-1} & w^{-1}z^{-1} & 1 \\ 3 & 1 & 1 & -z^{-1} & 0 \\ 5 & wz & 1 & -1 & -w \\ 7 & z & 0 & 1 & 1 \end{array}\right) \tag{9.5}$$

from which we compute the determinant

$$P(z,w) = w^{-1}z^{-1} + z^{-1} - w^{-1} - 8 + w + z + wz \tag{9.6}$$

This corresponds to the toric diagram of $\mathbf{dP}_3$ with multiplicity 8 for the central point. This result agrees with the Forward Algorithm computations in [13].

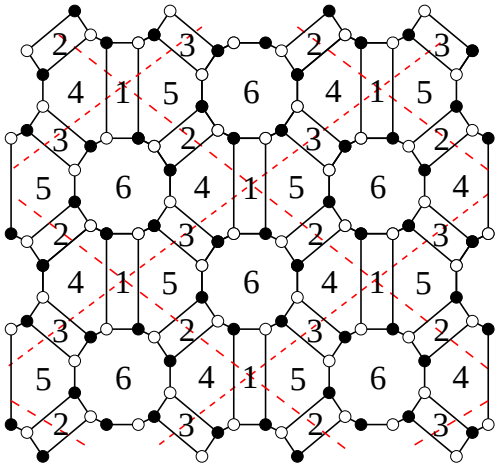

Figure 24: Brane tiling for Model IV of $\mathbf{dP}_3$.

Model IV

Figure 24 shows the brane tiling for this theory.

The Kasteleyn matrix is given by

$$K = \left(\begin{array}{c|cccccc} & 2 & 4 & 6 & 8 & 10 & 12 \\ \hline 1 & 1 & 0 & 0 & -wz & 0 & -1 \\ 3 & 1 & 1 & 0 & 0 & z & 0 \\ 5 & 0 & -1 & 1 & 0 & 0 & -w^{-1} \\ 7 & w^{-1}z^{-1} & 0 & 1 & 1 & 0 & 0 \\ 9 & 0 & -z^{-1} & 0 & -1 & 1 & 0 \\ 11 & 0 & 0 & w & 0 & 1 & 1 \end{array}\right) \tag{9.7}$$

and the characteristic polynomial is

$$P(z,w) = -w^{-1}z^{-1} - z^{-1} - w^{-1} + 11 - w - z - wz \tag{9.8}$$

Once again, this corresponds to the toric diagram of $\mathbf{dP}_3$. In this case, the multiplicity of the central point is 11, in agreement with the computations in [13].

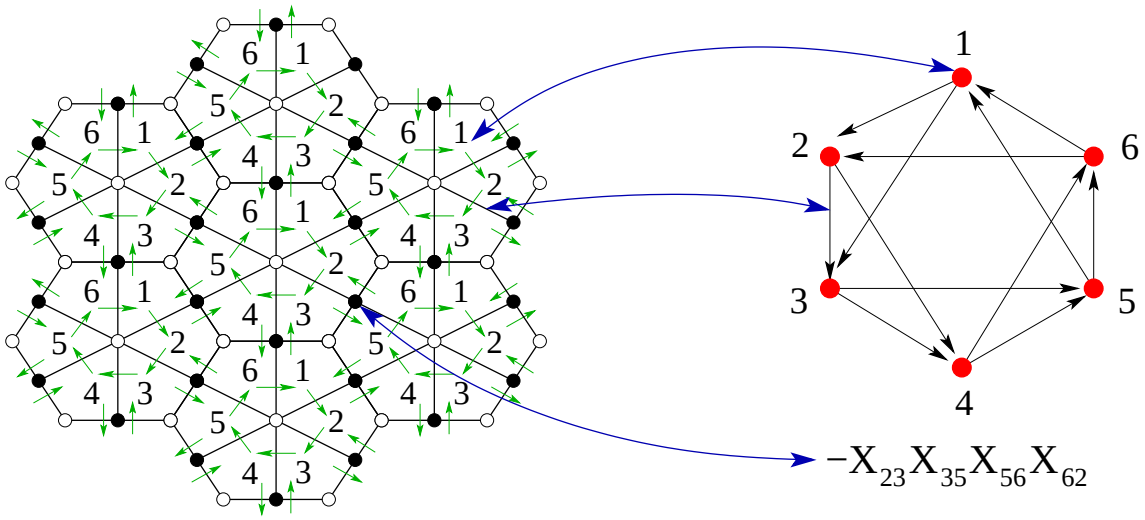

Figure 1: A finite region in the infinite brane tiling and quiver diagram for Model I of $\mathbf{dP}_3$. We indicate the correspondence between: gauge groups $\leftrightarrow$ faces, bifundamental fields $\leftrightarrow$ edges and superpotential terms $\leftrightarrow$ nodes.

data is to view it as defining a CW-complex; in other words, we may take the superpotential terms to define the 2-dimensional faces of the complex bounded by a given set of edges and vertices (the 1-skeleton and 0-skeleton of the complex). Thus, the quiver and superpotential may be combined into a single object, a planar tiling of a 2-dimensional (possibly singular) space. Toric quiver theories, as we will see, are defined by planar tilings of the 2-dimensional torus.

This is a key observation. Given the presentation of the quiver data (quiver graph and superpotential) as a planar graph tiling the torus, the bipartite graph appearing in the dimer model (the brane construction of the previous section) is nothing but the planar dual of this graph! Moreover, as we have argued, this dual presentation of the quiver data is *physical*, in that it appears directly in string theory as a way to construct the $3+1$-dimensional quiver gauge theory in terms of intersecting NS5 and D5-branes. The logical flow of these ideas is shown in Figure 2. Some of the concepts in this diagram have not yet been discussed in this paper, but will be addressed shortly.

Let us see how the properties of the brane tiling arise from those of the quiver theory. We will show that we can think of the superpotential and quiver together as a tiling of a two-dimensional surface, where bifundamentals are edges, superpotential terms are faces, and gauge groups are nodes. We refer to this as the "periodic quiver" representation. The toric condition, which states that each matter field appears in precisely two superpotential

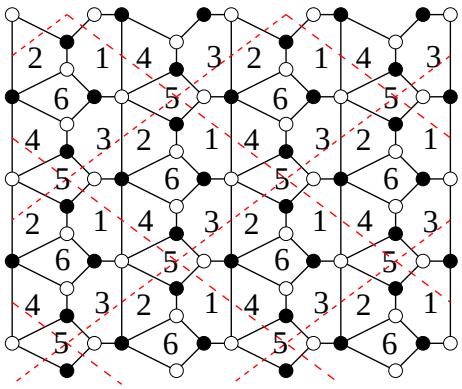

Figure 18: Brane tiling corresponding to the quiver diagram in Figure 17 and the superpotential in (8.1).

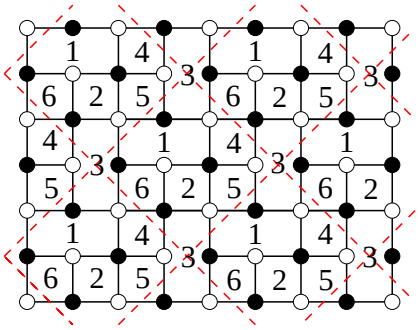

Figure 19: Brane tiling corresponding to the quiver diagram in Figure 17 and the superpotential in (8.2).

$$K_A = \left(\begin{array}{c|cccc} & 2 & 4 & 6 & 8 \\ \hline 1 & 1 & z^{-1} & 0 & w \\ 3 & -1 & 1 & 1 & 0 \\ 5 & z+w^{-1} & w^{-1} & 1 & -z \\ 7 & 1 & 0 & 1 & 1 \end{array}\right) \qquad K_B = \left(\begin{array}{c|cccc} & 2 & 4 & 6 & 8 \\ \hline 1 & 1 & 0 & w^{-1} & w^{-1} \\ 3 & z & 1 & 0 & w^{-1} \\ 5 & 1 & 1 & -1 & 1 \\ 7 & z & -1 & z & 1 \end{array}\right) \tag{8.3}$$

The corresponding characteristic polynomials are

$$P_A(z,w) = w^{-1}z^{-1} + z^{-1} - w^{-1} + 7 - w + z + wz \tag{8.4}$$

$$P_B(z,w) = -w^{-2} - 2w^{-1} - 1 - w^{-2}z + 7w^{-1}z - z - w^{-1}z^2 \tag{8.5}$$

From (8.4) and (8.5), we extract the toric diagrams shown in Figure 20.